A Feasible MPPT Algorithm for the DC/DC Boost Converter: An Applied Case for Stand-Alone Solar Photovoltaic Systems

Original Scientific Paper

Pham Hong Thanh
Thu Dau Mot University,
Electrical Engineering Program, Institute of Engineering and Technology
Thu Dau Mot City, Binh Duong Province, Vietnam
thanhph@tdmu.edu.vn

Le Van Dai*
Industrial University of Ho Chi Minh City,
Electric Power System Research Group, Faculty of Electrical Engineering Technology
Ho Chi Minh City, Vietnam
levandai@iuh.edu.vn
*Corresponded Author

Abstract *– One of the most promising forms of renewable energy is solar energy. However, efficient exploitation of this energy form is a topic of great interest, especially in obtaining the maximum amount of power from the solar photovoltaic (PV) system under changing environmental conditions. To solve this problem, it is necessary to propose an optimal algorithm. Therefore, this paper presents a feasible maximum power point tracking (MPPT) technique for DC/DC boost converters applied in load-connected stand-alone PV systems to extract the maximum available power. This proposed method is based on the combination of the modified perturb and observe (P&O) and fractional open circuit voltage (FOCV) algorithms. The effectiveness of the proposed technique is verified via time-domain simulation of the load-connected stand-alone PV system using PSIM software. The simulation results show a tracking efficiency with an average value of 99.85%, 99.87%, and 99.96% for tracking the MPP under varying loads, irradiation, and simultaneously varying temperature, load, and irradiation, respectively. In addition, tracking time is always stable at 0.02 sec for changing weather conditions in the large range. Therefore, the results of the proposed method indicate advantages compared to the conventional method.*

Keywords: *Maximum power point tracking (MPPT), perturb and observe (P&O), DC/DC boost converter, photovoltaic solar*

1. INTRODUCTION

According to the global market outlook, global installed PV capacity will increase to 940 GW by the end of 2021, a 22% increase from 772.2 GW in 2020, as shown in Fig. 1 [1]. Such a rapid increase is due to the ease of installation of this type of energy. For example, they can be installed in places without other uses, such as rooftops, deserts, or remote locations. Enhance, the development of PV energy has become a suitable research topic in the last decade. However, its power generation efficiency depends on the characteristics of the PV module, which vary with solar radiation level and atmospheric temperature [2]. To maximize energy from solar absorption at different radiation levels, the PV model must be driven at its maximum power point (MPP). In the past decade, a large number of MPP methods have been developed to increase the efficiency of the PV module.

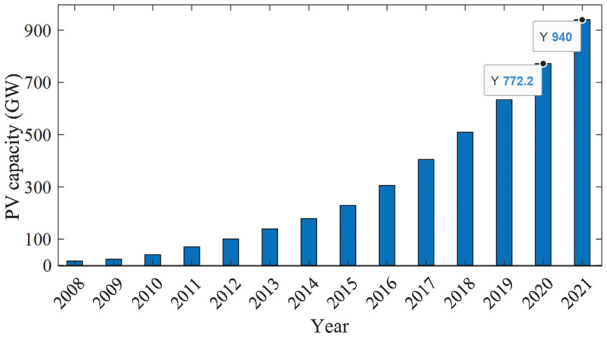

Fig. 1. Global growth in installed PV capacity 2008-2021

Currently, the PV power generation system can be divided into two types that are grid-connected and stand-alone PV systems. This paper focuses on the second type, which has been widely installed worldwide due to its low cost and high convenience in installa-

tion and use, especially for use in hard-to-connect or unconnected areas of the power grid. The stand-alone PV system refers to generating the electric energy that supplies the electrical load of the DC and AC types. This paper focuses on stand-alone PV, which is used to supply electric energy to a DC load. The architecture of the isolated-DC grid-connected PV system is proposed in this study, as shown in Fig. 2. This system can be divided into its key parts, which are the PV array, DC/DC boost converter, control unit, and load.

In this paper, the stand-alone photovoltaic solar system is considered to apply for any of the following: heating, cooking, and water pumping. For example, the authors in Ref. [3] have used this system to drive the pummel system using a brushless direct current motor. The battery is not used in this investigated system to save money and protect the environment. However, it has a significant problem in that the amount of the generated electric power depends on the weather conditions, especially solar irradiance. The efficiency of converting solar energy into electrical energy from PV panels is very low, usually in the range of 12% to 30%, due to the variations in irradiation, temperature, and load [4]. To enhance the conversion efficiency, the PV array should be tracked at the MPP. To achieve this goal, the MPP tracking (MPPT) algorithm for DC/DC converters is required. Basically, the MPPT algorithm is a power control method that adjusts the duty cycle of the DC/DC converter based on the output and input of the PV array to capture maximum power production continuously, thus achieving maximum power and supplying voltage stability under varying weather conditions.

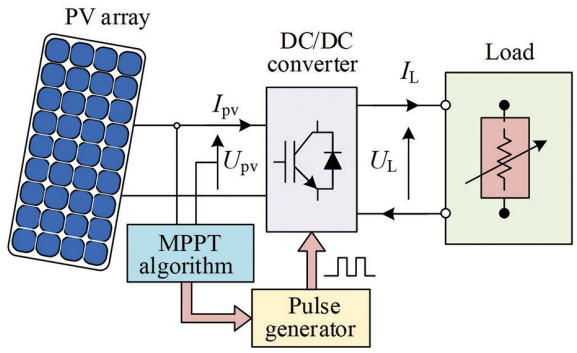

Fig. 2. The load-connected stand-alone PV system with the assistance of the MPPT algorithm

The MPPT algorithms are developed based on criteria including cost, efficiency, loss of energy, tracking time, level of oscillation, scientific tracking MPP, and type of power electric converter [5]. Considering these accounts, it has two MPPT algorithms. The first is conventional methods, which are simple and low-cost but lead to poor performance. The second has been developed using intelligent methods, which have high performance and are complex [6].

Over the last few years, there have been many proposed methods to achieve the MPPT under variable weather conditions. The most significant are methods such as perturb and observe (P&O) [7], incremental conductance (InC) [8], fractional open circuit voltage (FOCV) [9], and fractional short circuit current (FSCC) [10]. The use of these methods is effective; however, it has the problem of slow convergence and significant oscillations around the MPP. In addition, the PV array having the PV characteristic is not linear; thus, it needs to apply the MPPT control methods based on intelligent methods, including neural network (NN), fuzzy logic control (FLC), and the metaheuristic method. Authors in Ref. [11] have proposed the MPPT method based on the NN-global sliding mode for DC/DC buck-boost converter. The ANN-FL was developed by authors in Ref. [12]. The combination of the InC and FLC has been proposed by authors in [13]. These combination methods have several benefits, including being able to handle variable inputs, avoiding the requirement for precise mathematical modeling, and having self-convergence and self-learning capabilities [14]. The drawback of these methods is that the tracking performance and output efficiency are dependent on the engineer's technical knowledge. To overcome this problem, Manna, S et al. [15-18] introduced new methods based on the model reference adaptive control (MRAC) to enhance the tracking efficiency and speed of PV system under changes in ambient conditions. With these algorithms, it gives a reliable tracking efficiency and time compared to the traditional P&O, INC, FLC and ANF.

From an algorithmic point of view, even though the P&O algorithm has many benefits, a rapid change in atmospheric circumstances leads this P&O algorithm to drift away from MPP [19], and authors in Ref. [20] have provided analyses of this drift issue. In this study, the drift is clearly analyzed in terms of its potential occurrence, the movement of the operating point, and the effects of both abrupt changes in insolation and more gradual changes. As a solution to the drift issue, the authors in Ref. [21] have applied the constraint on perturbation step size (ΔD). However, the value of ΔD is high, resulting in an increase in steady-state power loss [22]. The adjustable variable step based on the Pythagorean theorem to calculate the reference voltage through the optimal value of ΔD is proposed by authors [23, 24]. However, it is manually adjusted to regulate this ΔD.

According to the literature survey, most are not interested in the self-adjusting optimal value ΔD under simultaneously varying temperature, load, and irradiation conditions. To solve this problem, this study proposes a solution that is based on the combination of the modified P&O and the FOCV algorithms. In this proposed algorithm, automatic tuning of the step size results in quick and precise tracking. Large perturbation values are better for improving dynamic performance, whereas lower values are better for improving steady-state performance. In addition, the proposed method also considers the drift problem early by setting upper and lower threshold limits for changes in power based on the slow and fast changes in the input of solar irradiance. The key contributions of this work are summarized as follows:

(i) The modeling of the load-connected stand-alone PV system designed using the PSIM environment and C++ code to assess the functionality of a PV module. This system, which consists of a PV array, a DC/DC boost converter, and an MPPT controller, can be used for any of the following: heating, cooking, and water pumping;

(ii) Establish a MPPT method based on the combination of the modified P&O and the FOCV algorithms to overcome the main drawbacks of the conventional P&O-MPPT.

(iii) The stability of the proposed method is confirmed under simultaneously changing radiation, temperature, and load.

Except for the introduction, this paper consists of four sections and is organized as follows: Section 2 covers the modeling, structure, and DC/DC boost converter. The principle of operation and the schematic diagrams of the DC/DC boost converter are presented in this section. Section 3 presents the control scheme for the DC/DC boost converter of the load-connected stand-alone PV system, followed by a recall of the conventional P&O-MPPT algorithm and a proposal for the modified P&O-MPPT algorithm. The effectiveness of the control method for the DC/DC boost converter based on the conventional and modified MPPT algorithms applied in stand-alone photovoltaic solar systems through other studied cases is verified, analyzed, discussed, and compared in Section 4. Finally, Section 5 contains the conclusions of this study, and the proposed directions for future research are presented in this section.

2. PROBLEM FORMULATION

2.1. PHOTOVOLTAIC ARRAY

The proposed single diode mode of the PV module in this study is shown in Fig. 3 and can be modeled by the relation between the output current and voltage as follows [2]:

$$I = I_{pv} - I_0\left(e^{\left(\frac{q}{\varsigma kT}(U+R_sI)\right)}-1\right)-\left(\frac{U+R_sI}{R_p}\right) \quad (1)$$

in which U is the output voltage, I is the output current, q is the electronic charge, ζ is the diode ideality factor, k is the Boltzmann constant, T is the operating temperature, R_s and R_p are respectively the series and parallel intrinsic resistances, I_{pv} is the photocurrent current and can determine by Eq. (2), and I_0 is the saturation current and can determine by Eq. (3)

$$I_{pv} = \left(I_{sc} + k_{sc}(T - T_r)\right) - \frac{\lambda}{1000} \quad (2)$$

$$I_0 = I_{rs}\left(\frac{T}{T_r}\right)^3 e^{q\frac{E_{bg}}{\varsigma k}\left(\frac{1}{T_r}-\frac{1}{T}\right)} \quad (3)$$

where λ is the illumination, E_{bg} is the band gap for silicon, k_{sc} is the short circuit factor, T_r is the reference temperature of the standard test conditions, and I_{rs} is the reverse saturation, which is given by the following equation.

$$I_{rs} = \frac{I_{sc}}{e^{\left(q\frac{U_{OC}}{\varsigma kT}\right)}-1} \quad (4)$$

where I_{sc} and U_{oc} are the short-circuit current and open-circuit voltage, respectively, which are respectively given as follows:

$$I_{sc} = \frac{G}{G_r}I_{sc.r} + k_i(T - T_r) \quad (5)$$

$$U_{oc} = U_{oc.r} + k_u(T_r - T) + \frac{\varsigma kT}{q}\ln\frac{G}{G_r} \quad (6)$$

where G and G_r are the actual solar radiation and the reference irradiance at the standard test conditions, respectively; $I_{sc.r}$ and $U_{oc.r}$ are the reference short circuit current and the reference open circuit voltage at the standard test conditions, respectively; and k_i and k_u are the temperature coefficient of I_{sc} and the temperature coefficient of U_{oc}, respectively.

For practical PV cells, the value of R_p is large leading to great influence when the PV operates in the current source region. Therefore, Eq. (1) can be reduced as follows:

$$I_{rs} = \frac{I_{sc}}{e^{\left(q\frac{U_{OC}}{\varsigma kT}\right)}-1} \quad (7)$$

In the case of a PV array having n_p parallel and n_s series of the PV cells connected together, the current can be described as follows:

$$I = n_pI_{pv} - n_pI_0\left(e^{\left(\frac{q}{\varsigma kTn_s}\left(U-\frac{n_s}{n_p}R_sI\right)\right)}-1\right) \quad (8)$$

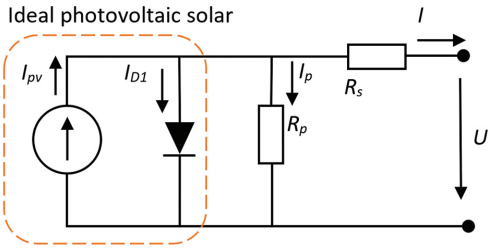

Fig. 3. The equivalent circuit of the PV module

2.2. DC/DC BOOST CONVERTER MODEL

2.2.1. Circuit description

The DC/DC converter used for the PV system includes the buck, boost, buck-boost, and single-ended primary-inductor converters. Based on their advantages, disadvantages, and applications [25, 26], the DC/DC boost converter is discussed and developed in many sectors, such as industrial drives, adaptive control, battery power applications, etc., compared to the other ones. Particularly in the case of the PV application, it not only the output voltage to the desired level but also performs the MPPT control. Therefore, DC/DC boost converter is chosen to study in this paper.

The MPPT-controlled PWM technique for the proposed stand-alone PV systems using the DC/DC boost

converter that is connected between the PV array and the load as shown in Fig.2. The equivalent circuit diagram is detailed in Fig. 4. The components are used, including the inductor L, power diode D_w, MOSFET *SW*, and capacitor C as shown in Fig. 4 (a).

Based on the time duration of *On* or *Off* for the *SW*, the DC/DC boost converter has two distinct modes of operation, including the continuous conduction operation (CCO) and the discontinuous conduction operation (DCO). For the CCO model, the current through L is always greater than zero, which means that the L partially discharges before the switching cycle begins. For the DCO model, the current through L goes to zero, which means that the L is fully discharged at the end of the switching cycle. Because the dynamic order of the converter is reduced, the DCO model was not selected compared to the CCO model [27]. Therefore, this study uses the CCO model for further study.

The process of recharging and discharge will constitute a switching cycle, standing for the obtained output voltage is controlled by the time duration of *On* or *Off* of *SW*. The PWM technique is applied to adjust the *On* or *Off* duration. The switching period of *SW* is T_w, the *SW* is closed with time $D_w T_w$ and open with $(1\text{-}D_w)$ T_w, in which D_w is the switching duty cycle. The performance of the boost converter depends on the input inductor and the connected load. The boost converter only operates in the case of $R_L \leq R_{MPP}$. Fig. 5 shows the tracking region of the boost converter on the *U-I* curve of the PV [28]. In order to attain the maximum power of the PV, the D_w must be changed so that the impedance values between the load and source are matched. So, the value of D_w is determined as follows [28, 29]:

$$D_w = 1 - \sqrt{\frac{R_{MPP}}{R_L}} \tag{9}$$

where R_{MPP} is the internal resistance of the PV array and R_L is load resistance.

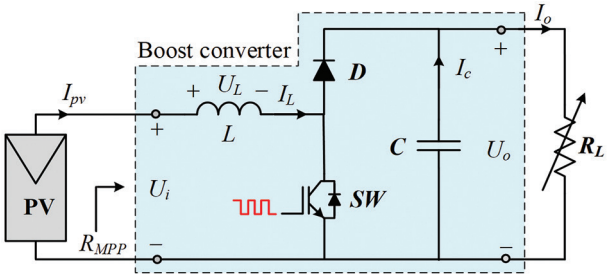

(a)

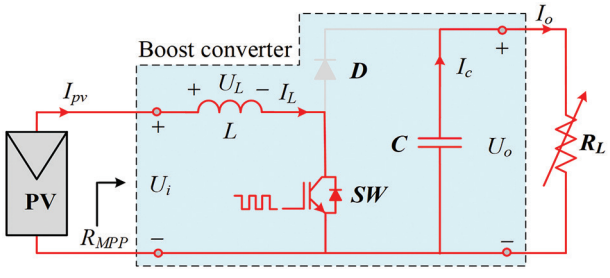

(b)

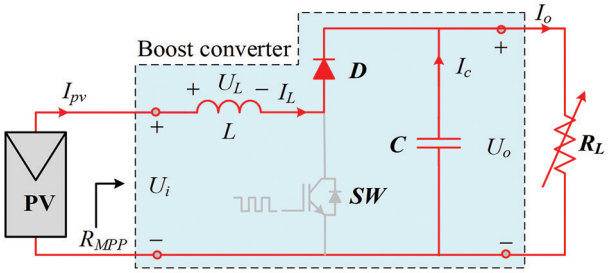

(c)

Fig. 4. The DC/DC boost converter: (**a**) The equivalent circuit representation, (**b**) Equivalent circuit in the case of turned-on switch *SW*, (**c**) Equivalent circuit in the case of turned-off switch *SW*

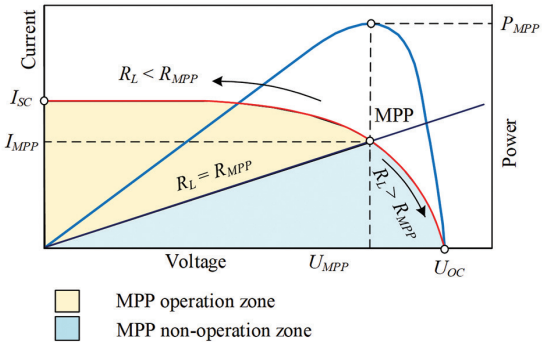

Fig. 5. Tracking region of the boost converter on the *U-I* and *P-U* curves of the PV

2.2.2. Operation analysis

The operation of this boost converter topology depends on the *On* or *Off* state of the switch *SW* and divides into two models.

Model # 1: It begins when the switch *SW* is turned on at time zero; the equivalent circuit is shown in Fig. 4 (b). During this model, the inductor L is connected to the ground, and the output voltage value is $U_o = U_i$. During this state, the inductor charged the energy. The current through the inductor L is raised and calculated by using Eq. (10). The load R_L is supplied the energy by the capacitor C. In this case, the diode current is equal to zero. The main operating waveforms of several components, in this case, are shown in the period $(0, D_w T_w)$ of Fig. 6.

$$I_L = \frac{1}{L}\int_0^{D_w T_w} U_i dt \tag{10}$$

Model # 2: It begins when the switch *SW* is turned off at the time of $D_w T_w$, the equivalent circuit is shown in Fig. 4 (c). During this model, the output voltage in the inductor L is changed and the value is $U_L = (U_o\text{-}U_i)$. During this state, the inductor discharged the energy through the diode to the load. The current through the inductor L is decayed and calculated by using Eq. (11). The main operating waveforms of several components, in this case, are shown in the period $(D_w T_w, T_w)$ of Fig. 6.

$$I_L = -\frac{1}{L}\int_{D_w T_w}^{T_w} (U_i - U_o) dt \tag{11}$$

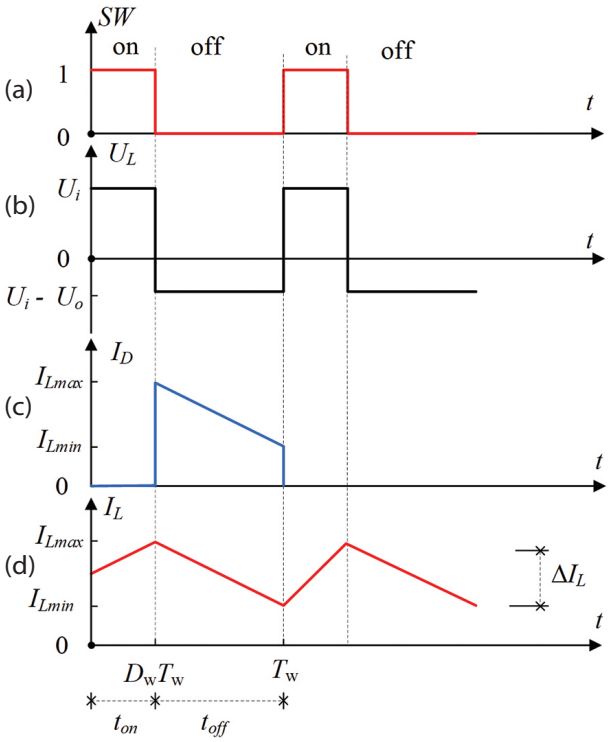

Fig. 6. Boost converter operating waveforms: (**a**) the switch *SW*; (**b**) Inductor voltage; (**c**) Diode current; (**d**) Inductor current

3. MPPT CONTROL METHOD

3.1. DC/DC BOOST CONVERTER

The equivalent circuit of the selected DC/DC boost converter is shown Fig. 4. The value of D_w is set up in the condition between zero to 1 and is considered in the condition without losses. The output voltage is calculated as follows [30]:

$$U_o = \frac{1}{1-D_w} U_i \tag{12}$$

The inductance value is determined by Eq. (13), and this value never falls to zero [31]:

$$L = \frac{(1-D_w)^2 D_w R_L}{2\Delta I_o f_w} \tag{13}$$

in which, ΔI_o is the output current ripple that is selected as 1% of the output current, and the switching frequency of f_w selected is the value of 20 kHz. The capacitance value is calculated as follows [32]:

$$C = \frac{U_o D_w}{\Delta U_o f_w R_L} \tag{14}$$

where ΔU_o is the output voltage ripple that is selected as 1%.

$$R_L = \frac{R_{MPP}}{(D_w - 1)^2} \tag{15}$$

where D_w is the switching duty cycle and can be determined as follows:

$$D_w = \frac{t_{on}}{(t_{on} + t_{off})} \tag{16}$$

3.2. MPPT ALGORITHMS

There are numerous MPPT algorithms for the DC/DC converter system based on solar energy systems that have been put out by numerous researchers with the shared objective of maximizing power output and operating the system at its maximum power point. The P&O is a widely popular technique for obtaining the most power from solar PV due to its ease of use and low cost in comparison to other MPPT techniques. Therefore, this paper considers this method to be improved and uses it as a new method.

3.2.1. Conventional P&O algorithm

The P&O method operates based on observing the PV power through the sensed values of the voltage and current of the PV array. Fig. 7 shows the principle of operation of this method, which depends on the calculation of the output power of the PV array based on the sensed values of the current and voltage. This power is compared to the previous one to address the direction of perturbation and, subsequently, update the switching duty cycle of the DC/DC converter as follows:

$$D_{w(k)} = D_{w(k-1)} \pm \Delta D_w \tag{17}$$

where $D_{w(k)}$ and $D_{w(k-1)}$ are the current and previous perturbations of D_w, respectively; k and (k-1) are the current and previous sampling instants.

In general, the PV array power is calculated based on the sensed values of the voltage and current. The values of voltage and power at k are stored as $P_{(k)} = U_{(k)} I_{(k)}$. Then, the power is calculated by using the previous values at (k - 1). The increment of the voltage and power of the PV array between two consecutive samples is determined as follows:

$$\begin{cases} \Delta U = U_{(k)} - U_{(k-1)} \\ \Delta P = P_{(k)} - P_{(k-1)} \end{cases} \tag{18}$$

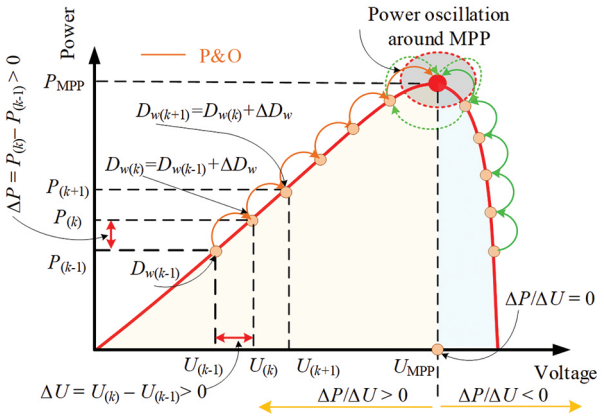

Fig. 7 . The principle of operation of the conventional perturb and observe algorithm

From Fig. 7, there are three conditions based on the fact that the slope of the power curve vs. voltage (current) of the PV array is zero at the MPP and can be described as follows:

i) $\frac{\Delta P}{\Delta U} > 0$: on the left of MPP, the voltage increases power increases;

ii) $\frac{\Delta P}{\Delta U} < 0$: on the right of MPP, power decreases with an increase in the voltage;

iii) $\frac{\Delta P}{\Delta U} = 0$: at MPP.

By comparing ΔP and ΔU, the algorithm decides whether to increase or decrease the duty cycle. If the voltage increases (positive) and the power increases (positive) in two consecutive calculation cycles, then the voltage will be driven to increase (positive) in the next cycle. If the voltage increases (positive), that leads to a decrease in power (negative), and then the voltage is controlled to decrease (negative) in the next cycle, and vice versa.

From Eq. (12), the output voltage is proportional to the D_w, which is determined by Eq. (16) and will be adjusted by increasing or decreasing a value called the "ΔD", and the updated values between two consecutive samples are determined by Eq. (17). This may be done repeatedly until the PMPP is achieved [33]. Table 1 lists the overall P&O direction characteristics, and Fig. 8 depicts its flowchart, which can be found in [34-35].

Table 1. The overall P&O direction characteristics

Voltage perturbation (ΔU)	Change in power perturbation (ΔP)	Direction of perturbation (ΔD_w)
+	+	+
+	-	-
-	+	-
-	-	+

3.2.2. Improved P&O algorithm

The conventional P&O algorithm has two main drawbacks. The first is that the ΔD_w is a fixed value, as shown in Fig. 7. This affects the process of achieving MPP because it depends on this ΔD_w jump. If this value is large enough to reach the MPP quickly, the system will fluctuate widely around the MPP. Conversely, if the offset is small, the system oscillates less around the MPP but takes longer to arrive at the MPP [36]. The second is that it depends on the measured voltage and current values, which depend on the sensors and measurement errors during the system's operation. For the measurement error, the system will measure the values n (usually choose a value from 3 to 7; if this value is too large, it is difficult to respond when environmental conditions change rapidly) times, then perform the comparison according to the P&O algorithm to find the trend in the next operating cycle [37].

To overcome these drawbacks, this study proposes a solution that the principle of operation of the proposed method is shown in Fig. 9 and the algorithm flowchart is shown in Fig. 10. In this proposed algorithm, automatic tuning of the step size results in quick and precise tracking. Large perturbation values are better for improving dynamic performance, whereas lower values are better for improving steady-state performance [37]. The current form of the generic tracking equation is presented in Eq. (17) above, in which the k^{th} optimum value of $\Delta D_{w(k)}$ should be determined as follows:

$$\Delta D_{w(k)} = M_{(k)}(grad\theta_{(k)}) \tag{19}$$

where $M_{(k)}$ is the k^{th} step size that is altered in accordance with the PV system's specifications. For this study, this value is calcaleted as follows:

$$M_{(k)} = \frac{P_{(k)}}{P_{(k-1)}} \tag{20}$$

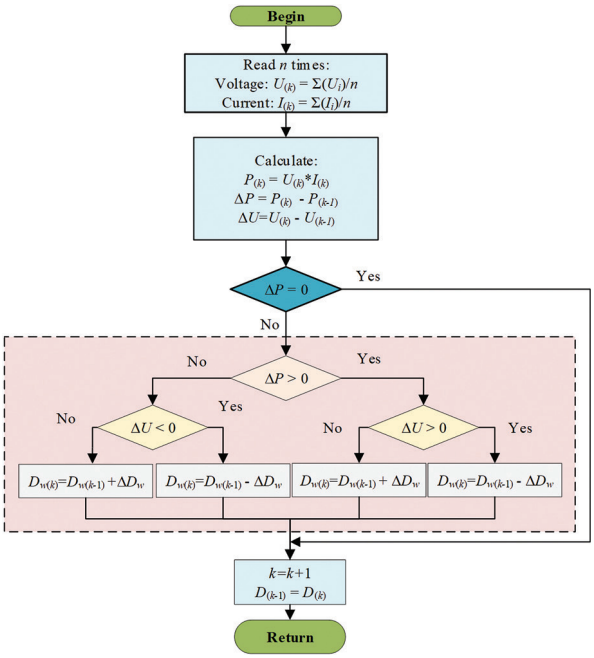

Fig. 8. The flowchart of the conventional algorithm

Corresponding to each working point of k^{th} of PV on the P-U characteristic curve as shown Fig. 9, the grad slope is determined as follows:

$$grad\theta_{(k)} = abs\left(\frac{\Delta P_{(k)}}{\Delta U_{(k)}}\right) \tag{21}$$

where $\Delta P_{(k)}$ and $\Delta U_{(k)}$ are the change in output power and working voltage of the PV module at the k^{th} step.

Substituting Eq. (19) into Eq. (17), and it can obtain as follows:

$$\begin{cases} D_{w(k)} = D_{w(k-1)} + M_{(k)}(grad\theta_{(k)}) & \text{(22a)} \\ D_{w(k)} = D_{w(k-1)} - M_{(k)}(grad\theta_{(k)}) & \text{(22b)} \end{cases}$$

It is clear from Eq. (22) that the modified automation complies with the operating point to provide a fast-tracking capability. As demonstrated in Fig. 9, when the operational point of the PV system is close to the MPP, the shift in the PV power and voltage is less significant than when the operational point is far from the MPP. As a result, the suggested approach boosts the MPPT tracker's speed during abrupt changes in the weather and lowers its oscillation during steady-state situations. Additionally, the suggested approach takes the drift issue into early consideration, Basically, the drift issue occurs when the solar

irradiation on the PV array rapidly increases by at least 10 Ws/m² [17]. The input of solar irradiance is thus dependent on the following two requirements for change in the solar irradiance perturbation ΔG_{STC} [38]

$$\begin{cases} \Delta G_{STC} < 10 \text{ is slow change} \\ \Delta G_{STC} > 10 \text{ is fast change} \end{cases} \quad (23)$$

Considering the irradiance of the PV system operating under standard test condition G_{STC} is 1000 W/m², the new conditions are obtained as follows:

$$\begin{cases} \dfrac{\Delta G_{STC}}{G_{STC}} < 1\% \text{ is slow change} \\ \dfrac{\Delta G_{STC}}{G_{STC}} > 1\% \text{ is fast change} \end{cases} \quad (24)$$

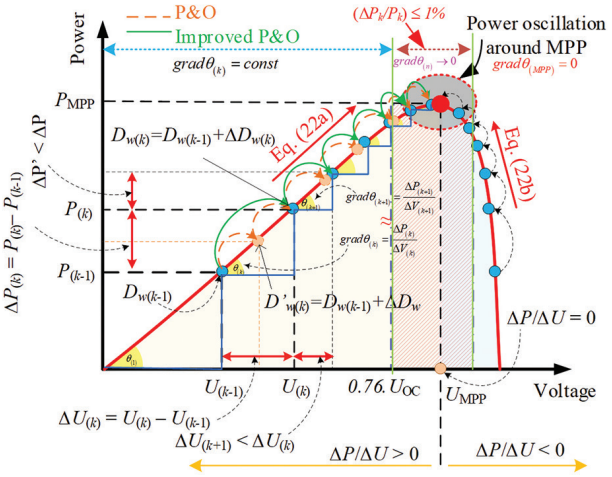

Fig. 9. The principle of operation of the proposed algorithm

The normalized change in solar irradiance is equivalent to the normalized change in power. Therefore Eq. (22) can be represented as [39]:

$$\begin{cases} \dfrac{\Delta P}{P} < 1\% \text{ is slow change} \\ \dfrac{\Delta P}{P} > 1\% \text{ is fast change} \end{cases} \quad (25)$$

where ΔP is the change in power and P represents its previous iteration. As known, if the irradiance varies and alters P's value, ΔP's value likewise changes in the same way. As a result, the value of $\Delta P/P$ remains essentially constant under a variety of environmental circumstances. Additionally, when the operation point is in the drift problem condition, this value is positive; otherwise, it is negative. In order to address the drift issue as soon as possible, a constant value of $\Delta P/P$ is inserted at the beginning of the program, as illustrated in Fig .10. In this paper, the value of $\Delta P/P$ is chosen as 0.01. Under various weather circumstances, the MPP voltage is computed at roughly 78% of the open circuit voltage. In order for the suggested method to determine the side of the operational point when the solar irradiance varies quickly, the U_{set} is applied as 76% of the open circuit voltage [39]. The operation point is to the right of the MPP if the PV voltage is greater than the U_{set}, which causes the D_w reference to decrease. If not, the D_w reference increases, and the $\Delta P/P$ shrinks dramatically when the operation point is near the MPP. As a result, the control unit enters the conventional P&O method to determine the precise optimum MPP.

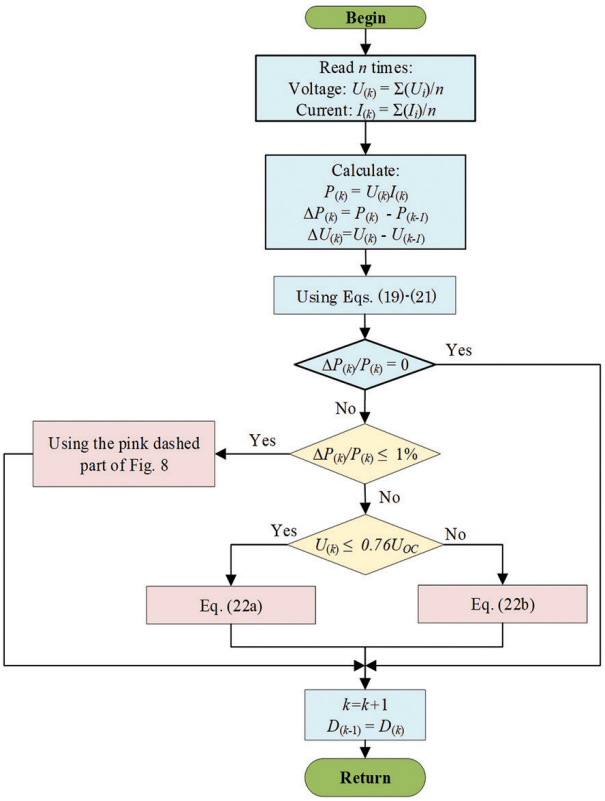

Fig. 10. The flowchart of the improved perturb and observe algorithm

4. RESULTS AND DISCUSSION

To assess the efficacy of the recommended method, a PSIM model for the proposed standalone PV system with MPPT algorithm has been developed, as shown in Fig. 11. A PV array, a DC/DC boost converter with an MPPT controller, and a resistive load are all components of the system under examination. Table 2 summarizes the electrical characteristics of the BP MSX 60 PV panel, which is used as a standard, under normal test conditions. The DC/DC boost converter design parameters are shown in Fig. 11 and were based on Section 3. The resistive load is adjustable and ranges in value from 50 Ω to 200 Ω.

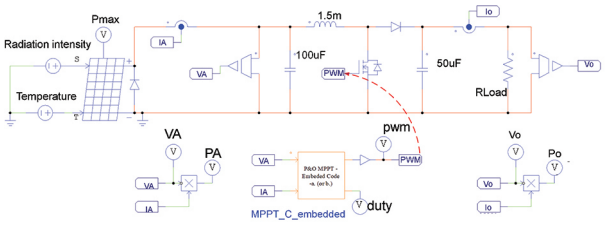

Fig. 11. Simulation model stand-alone photovoltaic system with MPPT algorithm

The *P-U* and *I-U* characteristics of a simulated BP MSX 60 PV panel for the irradiances of 200 W/m² and 1000

W/m² at 25 °C are shown in Fig.12. As a result, the MPP powers have changed from 10.66 W to 59.6 W, and the MPP voltages have changed from 16.88 V to 17.14 V corresponding to the insolation level of 200 W/m² and 1000 W/m², respectively.

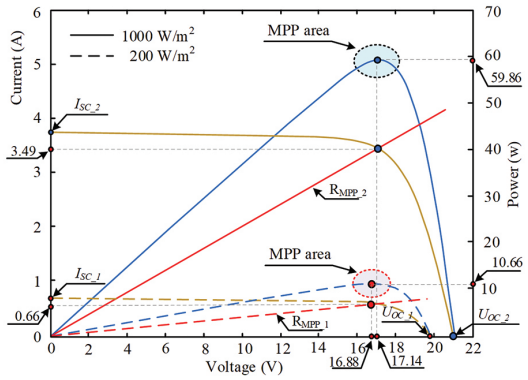

Fig. 12. The *I-U* and *P-U* characteristics for a module on the irradiances of 200 W/m² and 1000 W/m² at 25 °C

Table 2. Electrical characteristics of the PV module

Parameters	Values
The maximum power (Pmax)	60 W
The voltage at Pmax (Umpp)	17.1 V
The current at Pmax (Impp)	3.5 A
The open circuit voltage (Uoc)	21.1 V
The short circuit current (Isc)	3.8 A
The temperature coefficient of Uoc	-(80 ± 10) % V/°C
The temperature coefficient of Isc	-(0.065 ± 0.015) % V/°C
The temperature coefficient of power	-(0.5 ± 0.05) % V/°C
The nominal operating cell temperature	47 ± 2 °C
The operating temperature	25 °C

When the sun irradiation varies, it is not possible to manually adjust the load resistance with the variable value from 50 Ω to 200 Ω. Therefore, the MPPT algorithm and DC/DC boost converter have been designed in Section 3 to continuously adjust the duty cycle of the converter. Two scenarios are considered to verify the perfection of the proposed system.

Case 1: Simulation results for the varying load under the fixed irradiation: The tested system has been simulated for two predefined load levels of 100 Ω and 150 Ω. The fixed ambient temperature of 25 °C and the fixed irradiation of 1000 W/m² are considered inputs to the PV panel. Fig. 13 shows the comparison of the output power of the PV panel of both MPPT algorithms. Observing the dynamic response, the performance and efficiency of the proposed method are better in comparison with the conventional P&O algorithm in terms of response time and output power oscillations. The proposed method has a fine response and less fluctuation around the MPP than the conventional method. In the case of R_L = 100 Ω, it takes 0.05 seconds to reach the MPP point when applying the conventional MPPT method, whereas using the proposed MPPT method, it is 0.015 seconds, as shown in Fig. 13 (a).

In addition, a simulation for the predefined varying load is tested to verify the output response for the PV according to the following structure.

$$R_L(t) = \begin{cases} 100\Omega, & \text{for} \quad t \le 0.2 \text{ sec} \\ 50\Omega, & \text{for} \quad 0.2 \text{ sec} < t \le 0.5 \text{ sec} \\ 150\Omega, & \text{for} \quad 0.5 \text{ sec} < t \le 0.7 \text{ sec} \\ 200\Omega, & \text{for} \quad t > 0.7 \text{ sec} \end{cases} \tag{26}$$

The dynamic response is shown in Fig. 14, and the simulated results are summarized in Table 3. From this table, it can be seen that the proposed MPPT method presents better results than the conventional MPPT method in terms of response time, efficiency, and oscillations to reach the MPP point. The efficiency for tracking MPP is expressed by using Eq. (27) below, in which the maximum power is 60 W. As a result, the average efficiency and tracking time, in this case, are 99.85% and 0.0375 sec, respectively.

$$\eta = \frac{P_o}{P_{\max}} 100\% \tag{27}$$

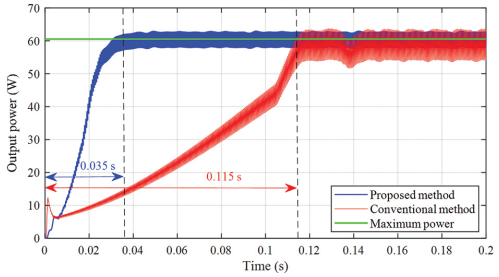

(a)

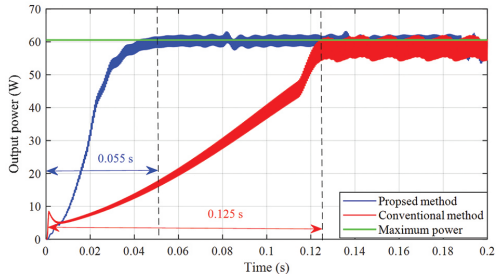

(b)

Fig. 13. The output power of a PV panel at 25 °C with the input irradiance of 1000 W/m²: (**a**) the load of 100 Ω, (**b**) the load of 150 Ω

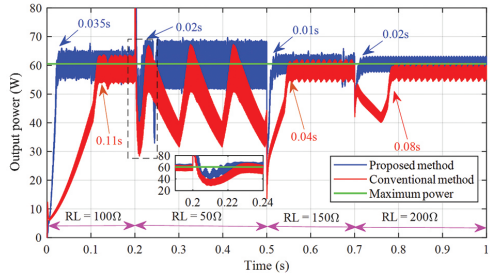

Fig. 14. The output power of a PV panel at 25°C with the input irradiance of 1000 W/m² under considering the predefined varying load

Table 3. A comparison of the properties of both methods for the predefined varying load and the fixed irradiation

Time (s)	R_L (Ω)	P_{max} (W)	Conventional algorithm			Proposed algorithm		
			P_o (W)	η (%)	Tracking time (s)	P_o (W)	η (%)	Tracking time (s)
0-0.2	50	60	49.01	81.68	0.11	59.89	99.82	0.03
0.2-0.5	100	60	58.80	98.00	0.11	59.92	99.87	0.03
0.5-0.7	150	60	58.20	97.00	0.11	59.91	99.85	0.04
0.7-1	200	60	57.64	96.07	0.09	59.92	99.87	0.05
Average	-	-	-	93.19	0.105	-	99.85	0.0375

Case 2: Simulation results for the varying irradiation under the fixed load: In this scenario, the input irradiation varies in a range of 200 W/m^2 to 1000 W/m^2 at the time from 0 to 1 second, the temperature operation is kept at 25°C, and the fixed load is 50 Ω according to the following structure.

$$\text{irradiance}(t)=\begin{cases}200\text{W/m}^2, & \text{for} \quad t\le 0.2\ \text{sec}\\ 1000\text{W/m}^2, & \text{for} \quad 0.2\ \text{sec}<t\le 0.4\ \text{sec}\\ 300\text{W/m}^2, & \text{for} \quad 0.4\ \text{sec}<t\le 0.6\ \text{sec}\\ (300\text{-}1000)\text{W/m}^2, & \text{for} \quad 0.6\ \text{sec}<t\le 0.8\ \text{sec}\\ 1000\text{W/m}^2, & \text{for} \quad t>0.8\ \text{sec}\end{cases} \quad (28)$$

The comparative output power of the two MPPT algorithms is shown in Fig. 15. According to the findings, the suggested method's power tracker addresses the input irradiance's correct direction, whereas the traditional method's tracking power does not when the input irradiation abruptly changes. Notably, the suggested approach's converter duty cycle caused the drift issue to affect the traditional method more than it did. In Fig. 16, this converter duty cycle is shown. Table 4 lists the simulated outcomes for both techniques. The efficiency for tracking MPP is expressed by using Eq. (27), in which the maximum power is defined by predefined power levels.

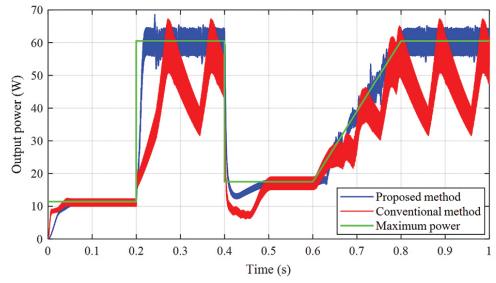

Fig. 15. The output power of a PV panel at 25°C with considering the varying irradiance

According to the results in Table 4, the proposed method's MPPT efficiency under all the different weather condition scenarios achieves an average tracking efficiency of 98.87% for the drift problem under sudden changes in weather conditions (suddenly increasing, suddenly decreasing, or linearly decreasing the input solar irradiation). The suggested strategy lowers the oscillation around the MPP under steady-state circumstances and swiftly follows the MPP during changes in weather, according to the findings of the simulations. In addition, compared to the typical approach, the output PV power is greater.

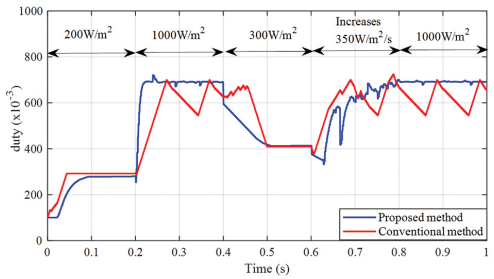

Fig. 16. The converter duty of a PV panel at 25°C with considering the varying irradiance

Case 3: Simulation results under simultaneously varying temperature, load, and irradiation: this scenario is carried out to verify the effectiveness of the proposed method for the PV system under different value range of the temperature, load, and irradiation for a period of 3 sec as shown in Fig. 17. The response of the output power of the PV system for each time when applying two method is shown in Fig. 18. The simulation results are summarized in Table 5.

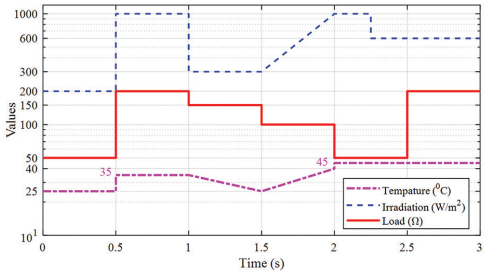

Fig. 17. The simultaneously varying temperature, load, and irradiation

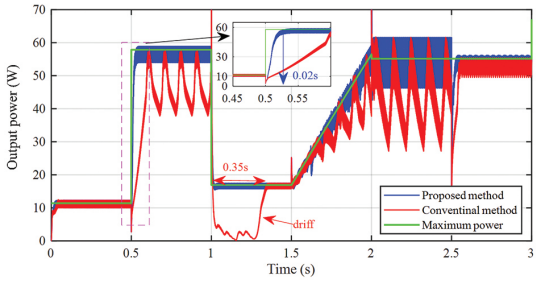

Fig. 18. The conveter duty of a PV panel under simultaneously varying temperature, load, and irradiation

Observing the obtained results shows that under different random changing conditions that affect the

survey system, the proposed method still achieves high tracking efficiency, with the lowest value of 99.71% and the highest up to 99.97%; the average efficiency in this case is 99.85%. The tracking time is always stable at 0.02 sec for condition of the large range of the temperature, load, and irradiation.

Contrary, the time is almost instantaneous (less than 0.005 sec). As a result, the proposed method gets better efficiency than the method of Ref [40]; the average efficiency under varying temperatures is 98.33 %, 96.475%, and 99.825% when applying FL, ANN, and ANN-fuzzy, respectively.

Table 4. A comparison of the properties of both methods for the fixed load and suddenly changed irradiation

Time (s)	*Irradiation (W/m²)*	P_{max} (W)	Conventional algorithm			Proposed algorithm		
			P_o (W)	η (%)	Tracking time (s)	P_o (W)	η (%)	Tracking time (s)
0 - 0.2	200	11.4	11.35	99.56	0.09	11.38	99.82	0.04
0.2 - 0.4	1000	60	50.00	83.33	0.30	59.93	99.88	0.015
0.4 - 0.6	300	17.49	17.32	99.03	0.11	17.48	99.94	0.07
0.6 - 0.8	300 - 1000	39.02	34.18	87.60	N/A	38.99	99.87	N/A
0.8 - 1.0	1000	60	50.00	83.33	N/A	59.91	99.85	N/A
Average	-	-	-	90.57	-	-	99.87	-

Table 5. A comparison of the properties of both methods under simultaneously varying temperature, load, and irradiation

Time (s)	P_{max} (W)	Conventional algorithm			Proposed algorithm		
		P_o (W)	η (%)	Tracking time (s)	P_o (W)	η (%)	Tracking time (s)
0-0.5	11.40	11.38	99.82	0.04	11.38	99.82	0.02
0.5-1.0	57.85	49.49	85.55	0.07	57.68	99.71	0.02
1.0-1.5	17.2	17.09	99.35	0.05	17.19	99.94	0.0015
1.5-2.0	37.53	32.87	87.59	N/A	37.49	99.89	N/A
2.0-2.3	55.16	47.21	85.58	0.02	55.05	99.80	0.005
2.3-2.5	32.96	29.78	90.35	0.002	32.93	99.91	0.002
2.5-3.0	32.95	29.11	88.35	0.04	32.94	99.97	0.02
Average	-	-	90.94	-	-	99.86	-

5. CONCLUSION

The marketability of photovoltaic solar energy will be heavily influenced by its efficiency, stability, and dependability. This paper has developed the control method for the DC/DC boost converter based on the MPPT algorithm applied in a stand-alone photovoltaic solar system in order to respond well and complete other renewable energy sources from a technical aspect. The main purpose is to improve the tracking efficiency, tracking speed, and oscillation related to changing the temperature, load, and irradiation, which are the main drawbacks of the conventional P&O-MPPT.

The PV panel type of the BP MSX 60 PV is considered when developing the mathematical model. The DC/DC boost converter is designed in accordance with the MPPT algorithm with the objective of maximizing power output and operating the system at its maximum power point. The design of the DC/DC boost converter and the modification of the conventional P&O-MPPT algorithm have been explained in deep detail. For the design of the DC/DC boost converter, the CCO model is applied. The constraint on perturbation step size is selected based on the impedance value between the load and source and is considered in the condition without losses. The inductance and capacitance values are calculated based on the output current, a voltage ripple of 1%, and a switching frequency of f_w set to 20 kHz. For the MPPT algorithm, it uses the modified perturb and observe (P&O) and fractional open circuit voltage (FOCV) algorithms to determine the duty ratio with an adaptive step size. In addition, a combination of current changes as well as power and voltage changes is considered in the decision-making process to avoid the drift problem early.

The simulation validation of the proposed and conventional P&O algorithms was presented and compared using study cases of varying loads under fixed irradiation and changing irradiation under a fixed load. The simulation results show that the proposed MPPT technique achieves efficiency with an average value of 99.85%, 99.87%, and 99.96% for tracking the MPP under varying loads, irradiation, and simultaneously varying temperature, load, and irradiation, respectively. The suggested strategy lowers the oscillation around the MPP under steady-state circumstances. It swiftly tracks the MPP during weather changes, according to the findings of the simulations. In addition, the output PV power is more significant compared to the conventional approach.

6. ACKNOWLEDGMENTS

This research is funded by Thu Dau Mot University, Binh Duong Province, Vietnam under grant number DT.21.1-068. The authors also appreciate the comments of reviewers and the support of Electric Power System Research Group, Industrial University of Ho Chi Minh City, Vietnam.

7. REFERENCES:

[1] S. Michael, "Global Market Outlook for Solar Power 2020-2026", https://www.solarpowereurope.org/insights/market-outlooks/global-market-outlook-for-solar-power-2022#downloadForm (accessed: 2022)

[2] M. G. Villalva, J. R. Gazoli, E. Ruppert Filho, "Comprehensive approach to modeling and simulation of photovoltaic arrays", IEEE Transactions on Power Electronics, Vol. 24, No. 5, 2009, pp. 1198-1208.

[3] B. Abdellahi, M. E. M. Mohamed Mahmoud, N. O. Dah, A. Diakité, A. El Hassen, C. Ehssein, "Monitoring the performances of a maximum power point tracking photovoltaic (MPPT PV) pumping system driven by a brushless direct current (BLDC) motor", International Journal of Renewable Energy Development, Vol. 8, No. 2, 2019, pp. 193-201.

[4] D. Sera, R. Teodorescu, P. Rodriguez, "PV panel model based on datasheet values", Proceedings of the IEEE International Symposium on Industrial Electronics, Vigo, Spain, 2007, pp. 2392-2396.

[5] N. Karami, N. Moubayed, R. Outbib, "General review and classification of different MPPT Techniques", Renewable and Sustainable Energy Reviews, Vol. 68, 2017, pp. 1-18.

[6] R. Alik, A. Jusoh, "An enhanced P&O checking algorithm MPPT for high tracking efficiency of partially shaded PV module", Solar Energy, Vol. 163, 2018, pp. 570-580.

[7] K. H. Hussein, I. Muta, T., Hoshino, M. Osakada, "Maximum photovoltaic power tracking: an algorithm for rapidly changing atmospheric conditions", IEE Proceedings-Generation, Transmission and Distribution, Vol. 142, No. 1, 1995, pp. 59-64.

[8] B. Liu, S. Duan, F. Liu, P. Xu, "Analysis and improvement of maximum power point tracking algorithm based on incremental conductance method for photovoltaic array", Proceedings of the IEEE 7th International Conference on Power Electronics and Drive Systems, Bangkok, Thailand, 27-30 November 2007, pp. 637-641.

[9] J. Ahmad, "A fractional open circuit voltage based maximum power point tracker for photovoltaic arrays", Proceedings of the IEEE 2nd International Conference on Software Technology and Engineering, San Juan, PR, USA, 3-5 October 2010, V1-247-V1-250.

[10] M. A. Masoum, H. Dehbonei, E. F. Fuchs, "Theoretical and experimental analyses of photovoltaic systems with voltage and current-based maximum power-point tracking", IEEE Transactions on Energy Conversion, Vol. 17, No. 4, 2002 pp. 514-522.

[11] I. U. Haq, Q. Khan, S. Ullah, S. A. Khan, R. Akmeliawati, M. A. Khan, J. Iqbal, "Neural network-based adaptive global sliding mode MPPT controller design for stand-alone photovoltaic systems", Plos One, Vol. 17, No. 1,2022 e0260480.

[12] E. Karatepe, T. Hiyama, "Artificial neural network-polar coordinated fuzzy controller based maximum power point tracking control under partially shaded condition", IET Renewable Power Generation, Vol. 3 No. 2, 2009, pp. 239-253.

[13] Y. N. Anagreh, A. Alnassan, A. Radaideh, "High Performance MPPT Approach for Off-Line PV System Equipped with Storage Batteries and Electrolyzer", International Journal of Renewable Energy Development, Vol. 10, No. 3, 2021, 507-515.

[14] S. Ullah, Q. Khan, A. Mehmood, S. A. M. Kirmani, O. Mechali, "Neuro-adaptive fast integral terminal sliding mode control design with variable gain robust exact differentiator for under-actuated quadcopter UAV", ISA Transactions, Vol. 120, 2022, pp. 293-304.

[15] S. Manna, D.K. Singh, A.K. Akella, H. Kotb, K.M. AboRas, H.M. Zawbaa, S. Kamel, "Design and implementation of a new adaptive MPPT controller for solar PV systems", Energy Reports, Vol. 9, 2023, pp.1818-1829.

[16] S. Manna, A. K. Akella, D. K. Singh,"A novel MRAC-MPPT scheme to enhance speed and accuracy in PV systems", Iranian Journal of Science and Technology, Transactions of Electrical Engineering, Vol. 47, No. 1, 2023, pp.233-254.

[17] S. Manna, D. K. Singh, A. K. Akella, A. Y. Abdelaziz, M. Prasad, "A novel robust model reference adaptive MPPT controller for Photovoltaic systems", Scientia Iranica, 2022.

[18] S. Manna, A. K. Akella, D. K. Si, D. K. Singh, "Implementation of a novel robust model reference adaptive controller-based MPPT for stand-alone and grid-connected photovoltaic system", Energy Sources, Part A: Recovery, Utilization, and Environmental Effects, Vol. 45, No. 1, 2023, pp. 1321-1345.

[19] D. P. Hohm, M. E. Ropp, "Comparative study of maximum power point tracking algorithms", Progress in photovoltaics: Research and Applications, Vol. 11, No. 1, 2003, pp. 47-62.

[20] D. Sera, L. Mathe, T. Kerekes, S. V. Spataru, R. Teodorescu, "On the perturb-and-observe and incremental conductance MPPT methods for PV systems", IEEE Journal of Photovoltaics, Vol. 3, No. 3, 2013, 1070-1078.

[21] N. Femia, G. Petrone, G. Spagnuolo, M. Vitelli, "Optimization of perturb and observe maximum power point tracking method", IEEE Transactions on Power Electronics, Vol. 20, No. 4, 2005, pp. 963-973.

[22] M. Killi, S. Samanta, "Modified perturb and observe MPPT algorithm for drift avoidance in photovoltaic systems", IEEE Transactions on Industrial Electronics, Vol. 62, No. 9, 2015, pp. 5549-5559.

[23] A. Charaabi, A. Zaidi, O. Barambones, N. Zanzouri, "Implementation of adjustable variable step based backstepping control for the PV power plant", International Journal of Electrical Power & Energy Systems, Vol. 136, p.107682.

[24] Y. Yang, F. P. Zhao, "Adaptive perturb and observe MPPT technique for grid-connected photovoltaic inverters", Procedia Engineering, Vol 23, 2011, pp. 468-473.

[25] S. Dahale, A. Das, N. M. Pindoriya, S. Rajendran, "An overview of DC-DC converter topologies and controls in DC microgrid", Proceedings of the IEEE 7th International Conference on Power Systems, Pune, India, 21-23 December 2017, pp. 410-415.

[26] M. H. Taghvaee, M. A. M. Radzi, S. M. Moosavain, H. Hizam, M. H. Marhaban, "A current and future study on non-isolated DC–DC converters for photovoltaic applications", Renewable and Sustainable Energy Reviews, Vol. 17, 2013, pp. 216-227.

[27] M. H. Rashid, "Power electronics handbook", Butterworth-Heinemann, 2017.

[28] O. P. Mahela, A. G. Shaik, "Comprehensive overview of grid interfaced solar photovoltaic systems", Renewable and Sustainable Energy Reviews, Vol. 68, 2017, pp. 316-332.

[29] P. V. Mahesh, S. Meyyappan, R. Alla, "Support Vector Regression Machine Learning based Maximum Power Point Tracking for Solar Photovoltaic systems", International Journal of Electrical and Computer Engineering Systems, Vol. 14, No. 1, 2023, pp. 100-108.

[30] A. J. Mahdi, S. Fahad, W. Tang, "An adaptive current limiting controller for a wireless power transmission system energized by a PV generator", Electronics, Vol. 9, No. 10, 2020, p. 1648.

[31] S. Fahad, A. J. Mahdi, W. H. Tang, K. Huang, Y. Liu, "Particle swarm optimization based DC-link voltage control for two stage grid connected PV inverter", Proceedings of the IEEE International Conference on Power System Technology, Guangzhou, China, 6-8 November 2018, pp. 2233-2241.

[32] S. K. Kollimalla, M. K. Mishra, "A novel adaptive P&O MPPT algorithm considering sudden changes in the irradiance", IEEE Transactions on Energy Conversion, Vol. 29, No. 3, 2014, pp. 602-610.

[33] K. L. Lian, J. H. Jhang, I. S. Tian, "A maximum power point tracking method based on perturb-and-observe combined with particle swarm optimization", IEEE Journal of Photovoltaics, Vol. 4, No. 2, 2014, pp. 626-633.

[34] T. Esram, P. L. Chapman, "Comparison of photovoltaic array maximum power point tracking techniques", IEEE Transactions on Energy Conversion, Vol. 22, No. 2, 2007, pp. 439-449.

[35] S. Jain, V. Agarwal, "Comparison of the performance of maximum power point tracking schemes applied to single-stage grid-connected photovoltaic systems", IET Electric Power Applications, Vol. 1, No. 5, 2007, pp. 753-762.

[36] G. C. Mahato, T. R. Choudhury, "Study of MPPT and FPPT: A brief comparison", Proceedings of the IEEE 17th India Council International Conference, New Delhi, India, 10-13 December 2020, pp. 1-7.

[37] L. Piegari, R. Rizzo, "Adaptive perturb and observe algorithm for photovoltaic maximum power point tracking", IET Renewable Power Generation, Vol. 4, No. 4, 2010, pp. 317-328.

[38] S. D. Al-Majidi, M. F. Abbod, H. S. Al-Raweshidy, "A novel maximum power point tracking technique based on fuzzy logic for photovoltaic systems", International Journal of Hydrogen Energy, Vol. 43, No 31, 2018, pp. 14158-14171.

[39] J. Ahmad, "A Fractional Open Circuit Voltage Based Maximum Power Point Tracker for Photovoltaic Arrays", Proceedings of the 2nd International Conference on Software Technology and Engineering, San Juan, PR, USA, 3-5 October 2010, pp. 247-250.

[40] L. Hichem, O. Amar, M. Leila, "Optimized ANN-fuzzy MPPT controller for a stand-alone PV system under fast-changing atmospheric conditions", Bulletin of Electrical Engineering and Informatics, Vol. 12, No. 4, 2023, pp. 1960-1981.